Current Research in Toxicology 1 (2020) 141–148

Contents lists available at ScienceDirect

Current Research in Toxicology

journal homepage: www.elsevier.com/locate/crtox

Histone deacetylase inhibitors prevent H_2O_2 from inducing stress granule formation

Siyuan Feng, Jennifer Nichole Daw, Qin M. Chen *

Department of Pharmacology, College of Medicine, University of Arizona, 1501 N. Campbell Ave, Tucson AZ85721, USA

ARTICLE INFO

Keywords:
Oxidative stress
Signaling transduction
Protein translation
Ribosomes
Cytoprotection

ABSTRACT

Reactive Oxygen Species (ROS) are generated as by-products of aerobic metabolism. The production of ROS increases during xenobiotic stress and under multiple pathological conditions. Although ROS are considered harmful historically, mounting evidence recently indicates a signaling function of ROS, preceding to and regulating transcriptional or post-transcriptional events, contributing to cell death or cell survival and adaptation. Among the cellular defense mechanisms activated by ROS is formation of stress granules (SGs). The stalled translational apparatus, together with mRNA, aggregates into microscopically detectable and molecularly dynamic granules. We found that with H_2O_2, the dose most potent for inducing SGs in HeLa cells is 400–600 μM. With 200 μM H_2O_2, 2 h treatment induced the highest percentage of cells containing SGs. Whether ROS signaling pathways regulate the formation of SGs was tested using pharmacological inhibitors. We probed the potential role of PI3K, MAPKs, PKC or histone deacetylation in SG formation. Using deferoxamine as a positive control, we found a lack of inhibitory effect of wortmannin, LY-294002, JNK-I, SB-202190, PD-98059, or H89 when the percentage of cells containing SGs was counted. About 35% inhibition was observed with HDAC6 inhibitor Tubastatin A, whereas general HDAC inhibitor Trichostatin A provided a complete inhibition of SG formation. Our data point to the need of investigating the role of HDACs in SG formation during oxidative stress.

1. Introduction

Multiple cellular defense mechanisms have evolved to deal with environmental and pathogenic stresses. Stopping protein synthesis in general serves to conserve energy yet avoid generating incorrect sequence or conformation of proteins. Upon cessation of protein translation, ribonucleoprotein complexes containing 40S ribosomes aggregate rapidly to form stress granules (SGs) for sheltering translation apparatus and mRNA species (Anderson and Kedersha, 2008; Kedersha et al., 2002; Buchan and Parker, 2009; Souquere et al., 2009; Protter and Parker, 2016; Panas et al., 2016). Over 150 proteins have been identified in SGs, including Ras GTPase Activating Protein Binding Proteins (G3BPs), Heterogeneous Nuclear Ribonucleoproteins (HNRNPs), ELAVL1, FUS and FUBP1 (Markmiller et al., 2018). Aggregation prone proteins such as T-Cell Intracytoplasmic Antigen-1 (TIA-1) and TIA-1 related protein (TIAR) are essential for SG formation (Kedersha et al., 1999; Gilks et al., 2004). Experimentally, SGs have been detected in tissues from diseases with increased oxidative stress, such as Amyotrophic Lateral Sclerosis, Alzheimer's, stroke and viral infection (Mahboubi and Stochaj, 2017; McCormick and Khaperskyy, 2017). Formation of SGs serves as a self-defense mechanism and a step for cell survival under oxidative stress.

Reactive oxygen species (ROS) are by-products of aerobic metabolism due to incomplete mitochondrial electron transport. An increase of ROS production has been observed from five sources: 1) environmental stress; 2) diseases involving inflammatory response; 3) ischemia and reperfusion; 4) metabolism of xenobiotics; and 5) alkylating agents or certain cancer chemotherapeutic agents, which deplete endogenous glutathione. At the molecular level, several endocrine factors and cytokines have been reported to induce ROS generation via mechanisms not completely understood, including Epidermal Growth Factor, Insulin, Angiotensin II, Tumor Necrosis Factor-alpha (TNF-α) and Interleukin-1β (Droge, 2002). With cells in culture, H_2O_2 serves well as a convenient tool for studying the consequence of oxidative stress.

ROS induce a plethora of signaling events to regulate various cellular endpoints. Many of these signaling events were first discovered as an immediate response to receptor binding of growth factors or endocrine factors (Sugden and Clerk, 2006). The common signaling events of ROS include activation of Phosphoinositide 3-Kinase (PI3K), Mitogen-Activated Protein Kinases (MAPKs), and Protein

* Corresponding author.
E-mail address: qchen@email.arizona.edu (Q.M. Chen).

https://doi.org/10.1016/j.crtox.2020.10.004
Received 14 July 2020; Revised 2 October 2020; Accepted 20 October 2020

Kinase C (PKC). The PI3K phosphorylates Akt, which in turn controls for cell survival response by inactivating pro-apoptotic molecule Bad and inducing pro-survival factor Bcl-2 (Barthel and Klotz, 2005). MAPKs have three branches: Extracellular Signal-Regulated Kinases (ERKs), c-Jun N-terminal Kinases (JNKs), and p38 MAPKs. Activation of ERKs is associated with cell survival response, while JNKs or p38 activation has been linked to apoptosis regulation in general (Matsuzawa and Ichijo, 2008). Family members of PKC are involved in signaling of cell growth, cell death and stress response leading to adaptation (Gopalakrishna and Jaken, 2000; Mochly-Rosen et al., 2012). Pharmacological inhibition of these kinases serves as the first step for understanding their participation in a specific cellular event.

Histone deacetylases (HDACs) can be an important regulator of ROS signaling and cellular response. Classic function of HDACs is enhancing binding of histones to DNA by removing acetyl groups from ε-N-acetyl lysine in histones. Nuclear HDACs regulate the expression of a long list of genes, including those encoding transcription factors, signaling molecules, and DNA repair enzymes. HDAC6, a cytosolic form of HDACs, can deacetylate α-tubulin, regulating microtubule assembly or stability. An increase activity of HDACs has been observed with induction of oxidative stress (Miura et al., 2008). Inhibitors of HDACs alter oxidative stress induced genes (Zelko and Folz, 2015). Previous work from our laboratory showed an association of HDAC6 with 40/43S ribosomes and HDAC6 inhibitor Tubastatin prevented stress induced protein translation (Kappeler et al., 2012). Because 40/43S ribosomes are an important component of SGs, the association of HDACs with this fraction supports a need to test the involvement of HDACs in SG formation. In this study, we characterized SG formation following induction of oxidative stress by H_2O_2, and address which signaling pathway is upstream of SG formation.

2. Materials and methods

2.1. Cell culture and treatment of H_2O_2 and pharmacological inhibitors

HeLa cells were maintained under tissue culture condition with weekly subculture in high-glucose Dulbecco's Modified Eagle's medium (DMEM) supplemented with 10% fetal bovine serum (FBS), 100 U/ml penicillin and 100 U/ml streptomycin. Cells were seeded into 24-well plates at 6.5×10^4 cells per well and reached 80% confluency before treatment with inhibitors and H_2O_2. Inhibitors were added to culture medium 1 h before H_2O_2 treatment.

2.2. Immunocytochemistry

Cells grown on glass coverslips were fixed in 4% formalin and washed two times with phosphate buffered saline (PBS) followed by additional wash with PBS containing 0.25% Triton X-100. Following 40 min incubation with blocking buffer [PBS containing 1% Bovine Serum Albumin (BSA) and 0.1% Tween 20], cells were incubated with the primary antibodies against TIA-1, S6 or L36 (Santa Cruz Biotechnology, CA, 1:100 dilution) for 1 h with shaking. After 5 washes with blocking buffer, the cells were incubated 1 h in dark with Alexa Fluor 488 or Alexa Fluor 568 conjugated secondary antibody (Invitrogen Molecular Probes, CA, 1:600 dilution). After removal of unbound antibody by 5 washes in PBS, the coverslips were mounted onto a microscopic slide with Vectashield Antifade Mounting Medium (Vectashield Laboratories, CA). Images were acquired with Olympus fluorescence microscope under 60x or 100x oil objective lenses.

2.3. Stress granule counting and statistical analysis

Cells and SGs were randomly selected for counting. To measure the percentage of cells containing SGs, about 300 cells were counted under a 60× objective lens. To determine the number of SGs per cell, SGs were counted from 20–100 cells under 100x objective lens. The diameters of 60 SGs were measured under 100× objective lens with "arbitrary line" tool of the Olympus CellSens Standard software. Two-tail Student's *t* test or one way ANOVA was used to measure the significance of data sets. A value of $p < 0.05$ was used to determine the statistical significance.

2.4. MTT assay

Cells were seeded at a density of $3x10^4$ per well in a 24-well plate containing 1 mL culture medium. When reaching 80% confluency, cells were treated with H_2O_2 for 2 h and placed in fresh medium for additional 16 or 24 h of culture. MTT was added to the culture media to a final concentration of 0.16 mg/mL. Following 30 min incubation in a tissue culture incubator at 37 °C with 5% CO_2, purple crystals of reduced formazan were observed inside cells under a phase contrast microscope. The culture medium was removed and the formazan crystals were dissolved in isopropanol containing 4 mM HCL and 0.1% NP-40 for measuring cellular metabolic state by comparing the absorbance at 570 nm.

3. Results

3.1. SG formation during oxidative stress

SGs are commonly viewed as stalled translation complexes containing mRNAs, 40S ribosomes, eukaryotic Initiation Factors (eIFs), poly A binding proteins (PABPs), and additional RNA binding proteins. It is thought that either eIF2 α phosphorylation or non-translating mRNA can prepare the core containing pre-initiation complex, i.e. 40S ribosomes plus mRNA, eIFs and the polyA binding protein, into the origin of a membrane-free SG structure. This core recruits aggregation-prone proteins, such as TIA-1/TIAR, to form SG seed. Fusion of the seeds along microtubules produces microscopically visible SGs (Panas et al., 2016). TIA-1 is an RNA-binding protein containing a prion-like domain necessary for formation of SGs (Gilks et al., 2004). Immunocytochemistry staining for TIA-1 represents a standard method for detection of SGs in the cytoplasm. Since SGs contain the 40S small subunit of ribosome due to the fact that SGs are derived from stalled translation initiation complex, we validate the specificity of TIA-1 staining for SGs by co-localization study. H_2O_2 indeed induces SG formation (Fig. 1A) and colocalization of TIA-1 with small ribosomal subunit protein S6 (Fig. 1B) but not large ribosomal subunit protein L36 (Fig. 1C), supporting the specificity of TIA-1 staining for SGs.

Dose response studies were performed to define the dose range of H_2O_2 for SG formation. An early report had shown that H_2O_2, when added to cells in culture, disappears in culture medium in a dose and time dependent manner. With one million cells treated with 100 or 200 μM H_2O_2, about 90% H_2O_2 were eliminated from the culture medium within 60 mins (Yakes and Van Houten, 1997). This means that by 2 h, the majority if not all H_2O_2 has been depleted by cells. For cells treated 2 h with non-lethal doses of H_2O_2, i.e. 100, 200, 300, 400, 600 or 800 μM (Fig. 2A), we found that 400–600 μM H_2O_2 caused SG formation in 80% cells, whereas a higher dose, i.e., 800 μM H_2O_2 is not as effective for inducing SG formation, caused the percentage of cells containing SGs to a level similar to that of 300 μM (Fig. 2B). Among the cells containing SGs, the number of SGs per cell does not appear to change significantly from dose to dose (Fig. 2C). Metabolic activities of the cells were measured by MTT assay at 2 h and 24 h after H_2O_2 treatment to show that SGs form at the doses, i.e. 200–400 μM, which do not suppress the metabolic activity of the cells significantly, when the SGs are detectable within 2 h of H_2O_2 treatment, or even after 24 h. Although morphologically cells appeared normal at high doses of H_2O_2, i.e. 600–800 μM, the metabolic activity as measured by MTT absorbance declined (Fig. 2D), cor-

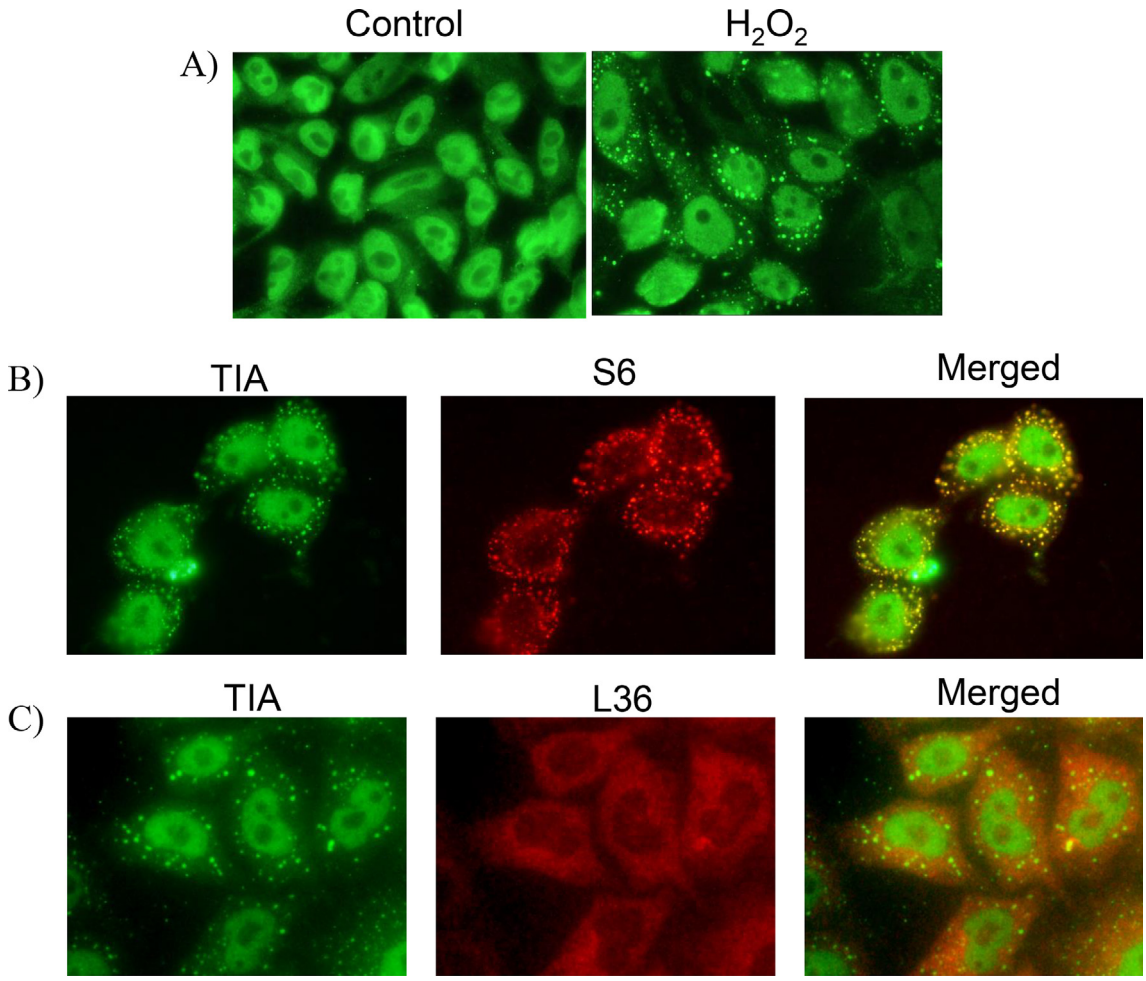

Fig. 1. H_2O_2 Induced Formation of Stress Granules in Hela cells. HeLa cells grown to 80% confluency on glass coverslips were exposed to 400 μM H_2O_2 for 2 h before immunocytochemistry. Stress granules (SGs) were detected by immunocytochemistry staining for TIA-1 with Alexa Fluor 488 conjugated secondary antibody (A). For dual staining, cells were stained with TIA-1 first before immunocytochemistry staining for S6 or L36 protein using Alexa Fluor 568 conjugated secondary antibody (B, C).

relating with less than optimal dose for SG formation. When the dimension of SGs were measured with various doses of H_2O_2 treatment, we observed a dose dependent increase in the size of SGs from 100 to 300 μM H_2O_2, with the overall size of SGs being the biggest with 300 μM H_2O_2 treatment (Fig. 3B).

To determine how soon or time dependence of SG formation, we treated cells with 200 μM H_2O_2 for 0.5, 1, 2, 4, 8, 12 and 24 h, then counted the percentage of cells with SGs versus the number of SGs per cell. A time dependent increase of the percentage of cells containing SGs was observed within the first 2 h, with SG first detectable at 0.5 h and fewer cells containing SGs after 2 h (Fig. 2B). The number of SGs per cell showed significant increase at 0.5 h and maintained for 2 h (Fig. 2C). The trend showed a decrease in the number of SGs per cells in those cells containing SGs after 2 h. By 24 h, most SGs had disappeared based on the percentage of cells containing SGs or the number of SGs per cell (Fig. 4A-C).

3.2. Pharmacological inhibition of SG formation

Oxidants are known to activate a plethora of signaling events, and inhibitors of these signaling pathways are available for testing the involvement of PI3K/Akt, MAPKs, PKCs and HDACs. Deferoxamine (50 μM) was included as a positive control, which chelates iron and blocks formation of reactive hydroxyl radical from H_2O_2. Previous work from our laboratory showed that PI3K/Akt was inhibited by Wortmannin (40 μM) and LY294002 (40 μM) (Tu et al., 2002), whereas MAPKs were inhibited by JNK inhibitor I (JNK-1, 12 μM, for JNKs), SB202190 (30 μM for p38) and PD98059 (80 μM for ERKs) (Barr et al., 2004; Davies et al., 2000; Tu and Chen, 2003; Coronella-Wood et al., 2004). H89 (30 μM) is a widely used general inhibitor of protein kinase C. Tubastatin A (10 μM) is a potent inhibitor with high specificity for HDAC6 (Kappeler et al., 2012; Butler et al., 2010). Trichostatin A (10 μM) is a general inhibitor of HDACs and has a broad spectrum of activity reducing function of HDACs (Drummond et al., 2005).

Without H_2O_2 treatment, some inhibitors caused an increase in the number of cells containing SGs, such as LY294002, SB202190, and H89 (Fig. 5A). The effect of H89 in inducing the fraction of cells containing SGs or the number of SGs per positive cell is most dramatic, over 7 fold compared to the control without any drug treatment (Fig. 5A&B). H89 caused significant inhibition of cellular metabolism (Fig. 5C). In contrast, Trichostatin A did not induce SG formation despite of inhibition of cell metabolism as measured by MTT (Fig. 5C).

With H_2O_2 treatment, Deferoxamine showed a complete blockage of SG formation (Fig. 5A). While Tubastatin A showed about 35% inhibition when the percentage of cells containing SGs was counted, Trichostatin A completely blocked H_2O_2 from inducing SG formation based on the percentage of cells containing SGs (Fig. 5A). When the number of SGs per cell was counted in those cells containing SGs, the inhibitors did not significantly affect this measure, even with Deferoxamine or Trichostatin A. A downward trend in the number of SG per cell was observed with LY294002 and SB202190 for H_2O_2

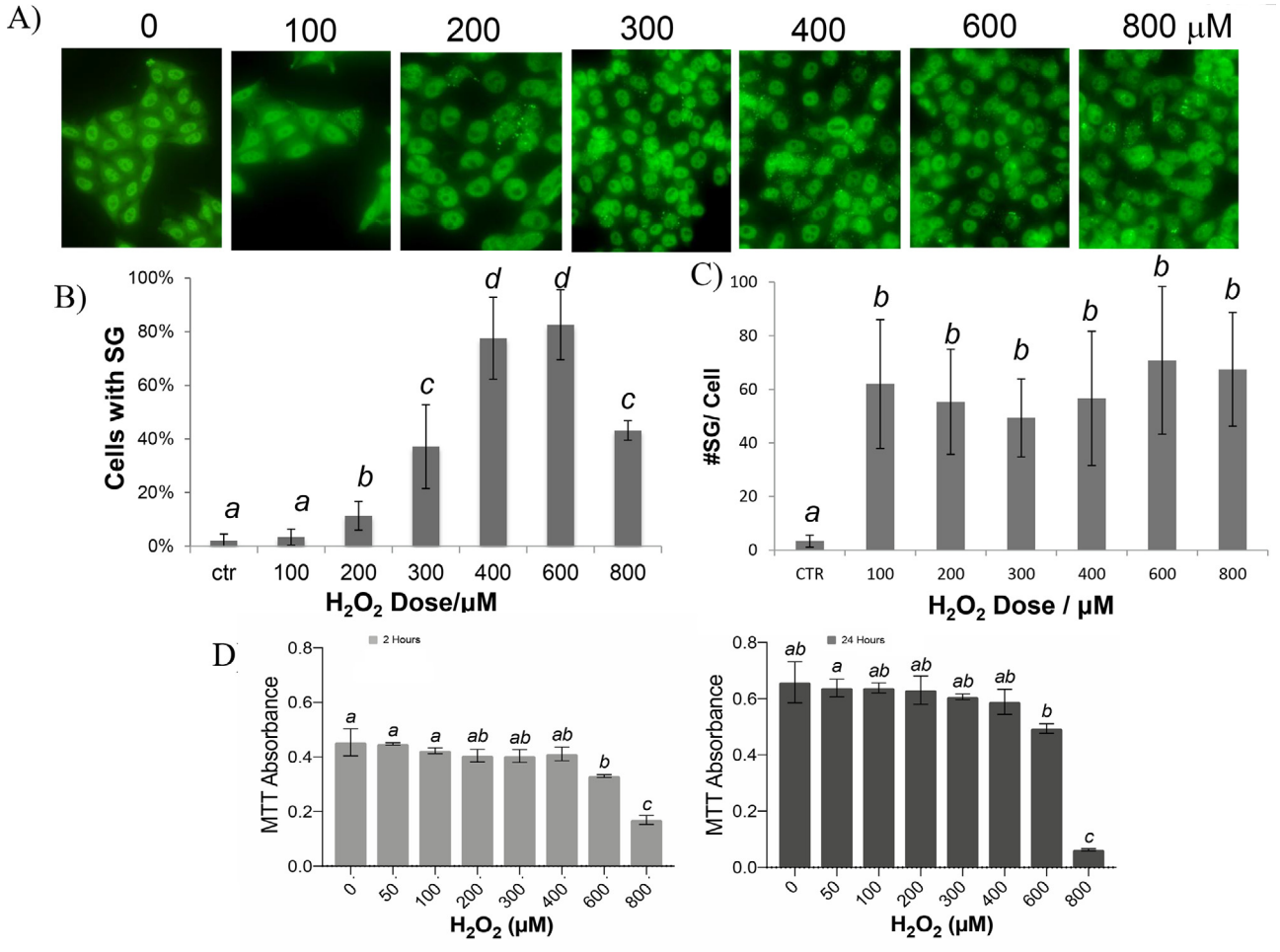

Fig. 2. H_2O_2 Dose Dependent Induction of Stress Granules and Metabolic Inhibition. HeLa cells grown to 80% confluency on glass coverslips were exposed to 0, 100, 200, 300, 400, 600 or 800 μM of H_2O_2 for 2 h. Following fixation, immunocytochemistry was performed for TIA-1 staining and fluorescence microscopy (A). Under a fluorescence microscope with 60 × lens, we counted about 300 cells in random fields to determine the percentage of cells containing SGs (B). About 100 cells containing SGs were picked for counting the number of SGs per cell under a 100 × objective lens (C). MTT assay was performed at 2 h or 24 h after H_2O_2 treatment as described in the Methods (D). The data obtained from 3 replicates of one experiment representative of three were used for statistical analysis by ANOVA. Different letters indicate a significant difference between groups ($p < 0.05$). The mean labeled with "*a*" is significantly different from the means labeled with "*b*", "*c*" or "*d*", whereas "*ab*" indicates no significant difference between "*a*" or "*b*".

treated cells compared to the cells treated with H_2O_2 without inhibitors (Fig. 5B).

The inhibitory effect of Trichostatin A on SGs was detected when cells were exposed to H_2O_2 for 2 h. If an inhibitor blocks cytotoxic effort of H_2O_2, such as with Deferoxamine, an inhibition of SG formation is expected. To excluding the possibility that Trichostatin A blocks SG formation due to inhibition of H_2O_2 cytotoxicity, MTT assay was performed to confirm Trichostatin A did not affect metabolic inhibition or cytotoxicity of high dose H_2O_2 (Fig. 5C). At 16 h after 800 μM H_2O_2 treatment, although Deferoxamine prevented H_2O_2 from metabolic inhibition, Trichostatin A failed to do so. These data suggest that the inhibitory effect of Trichostatin A on H_2O_2 induced SG formation is independent of cytotoxicity inhibition.

4. Conclusion

Our data indicate that formation of SGs as a result of H_2O_2 exposure is a dynamic process, depending on the dose as well as the time frame of stress. The optimal dose for SG induction is 400–600 μM. The time point for the highest level of SGs is 2 h of H_2O_2 exposure. Among the signaling pathways of oxidative stress, inhibition of HDACs appears to prevent SG formation.

5. Discussion

The time frame of SG formation observed here is consistent with a live cell imaging study (Martin and Tazi, 2014). The process of SG assembly or de-assembly appears to be ATP driven since ATP-dependent disaggregases, DEAD-box helicases and autophagy proteins have been found in SGs (Jain et al., 2016). Autophagy of SGs, a process termed granulophagy, consists a mechanism of SG removal, providing one explanation for the disappearance of SGs over time (Buchan et al., 2013). In addition, cells may resume translation through converting SGs to processing bodies, i.e. P bodies, for disassembly of the granular structure and decaping RNA for translation initiation (Protter and Parker, 2016). Therefore, SGs serve to control the timing of protein translation in addition to protection of RNA and translational machinery.

Not all forms of stress can induce SGs. Some of the pharmacological inhibitors such as LY-294002 and Trichostatin A, while exhibited cytotoxicity and inhibit cellular metabolism, did not induce SG formation (Fig. 5). In contrast, H89, an inhibitor of PKC, was an effective inducer of SGs for a mechanism yet to be determined (Fig. 5). While inhibition of cellular metabolism was observed with H89, H89 did not affect SG induction by H_2O_2, arguing against a role of PKC in H_2O_2 induced SG

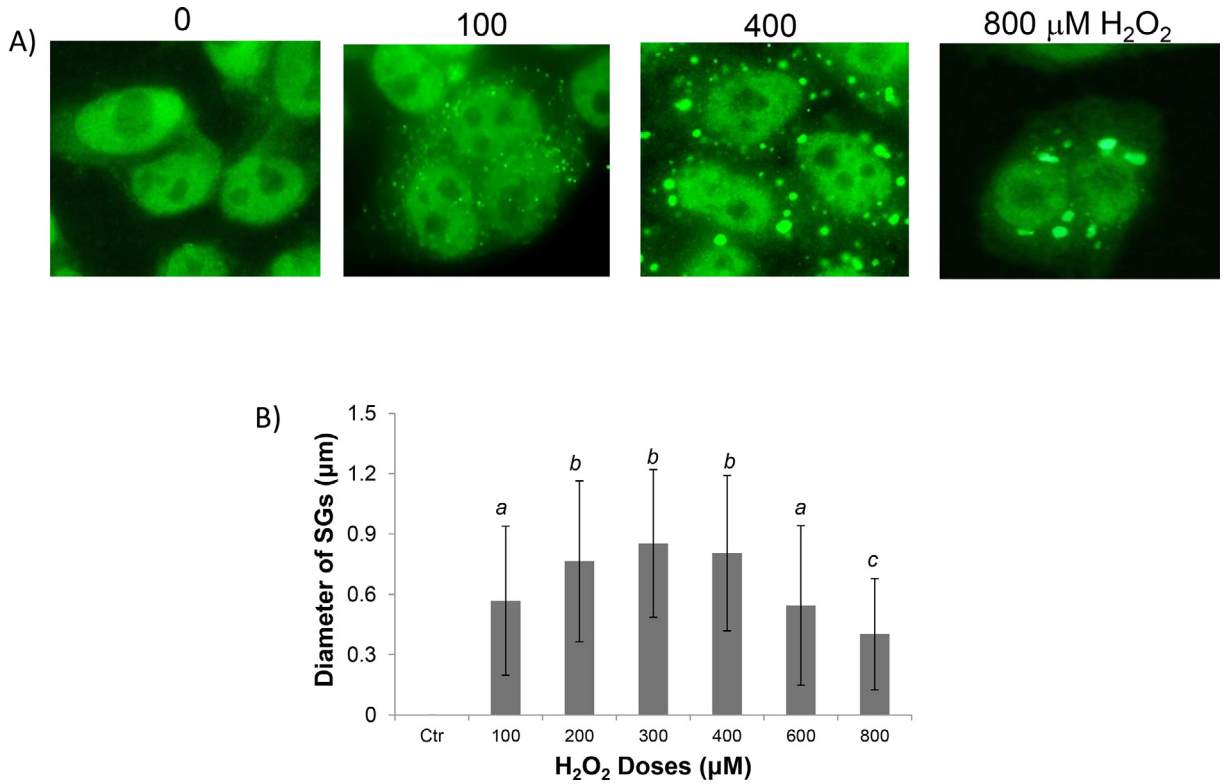

Fig. 3. H_2O_2 Dose Dependent Changes in the Size of Stress Granules. HeLa cells grown to 80% confluency on glass coverslips were exposed to 0, 100, 200, 300, 400, 600 or 800 μM of H_2O_2 for 2 h. Following fixation, immunocytochemistry was performed for TIA-1 staining. The size differences of SGs were shown with representative images (A). The diameters of 60 SGs were measured under 100x objective lens with "arbitrary line" tool of the Olympus CellSens Standard software, and were presented as average ± standard deviations (B). The diameters of 60 SGs were used for statistical analysis by Student's *t*-test assuming unequal variances. Different letters indicate significant differences between the groups ($p < 0.05$). The means labeled with "*a*" are significantly different from that labeled with "*b*" or "*c*", whereas "*b*" indicates significant difference from that labeled "*a*" or "*c*".

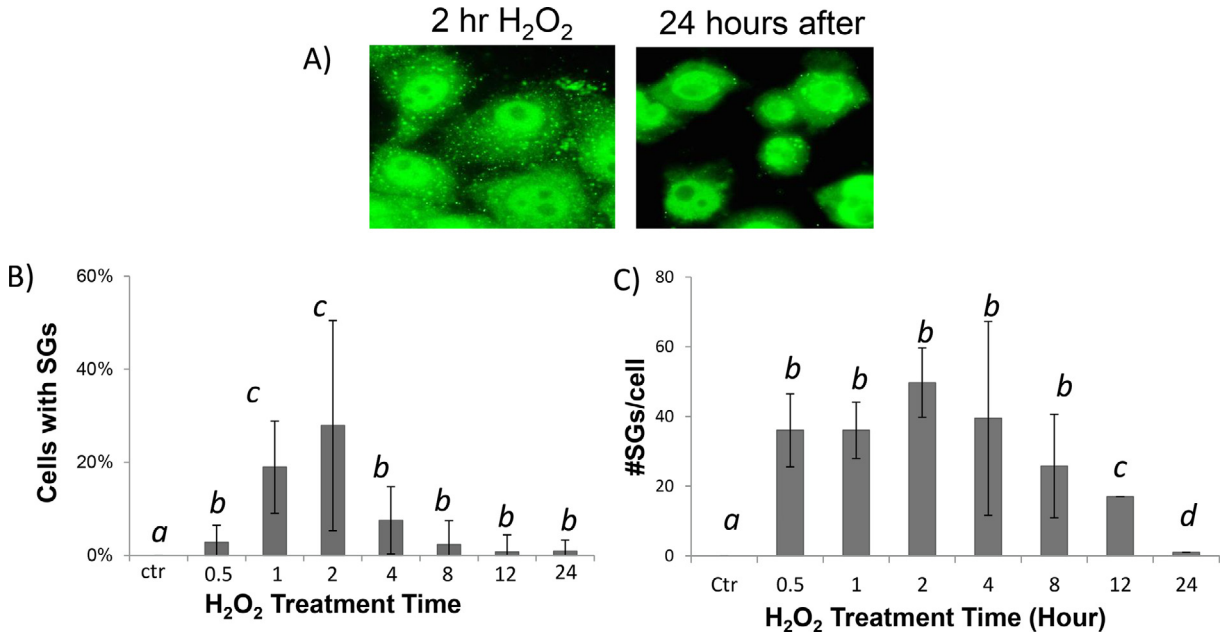

Fig. 4. Time Dependency of Stress Granule Formation. HeLa cells were treated by 200 μM of H_2O_2 for 0.5, 1, 2, 4, 8, 12 and 24 h. For 4, 8, 12, 24 h time points, cells were incubated with H_2O_2 for 2 h, before culture medium was replaced with fresh DMEM containing 10% FBS. Cells were fixed for immunocytochemistry of TIA-1 staining. Representative images from 2 h or 24 h are shown (A). About 300 cells in random fields were counted from each sample under a 60 × objective lens for determining the percentages of cells containing SGs (B). For measuring the number of SGs per cell, 60 cells containing SGs were picked for counting the number of SGs per cell under a 100 × objective lens (C). The data obtained from 3 replicates or 60 cells were used for statistical analysis by ANOVA (A, B). Different letters indicate a significant difference between groups ($p < 0.05$). The mean labeled with "*a*" is significantly different from the means labeled with "*b*", "*c*" or "*d*".

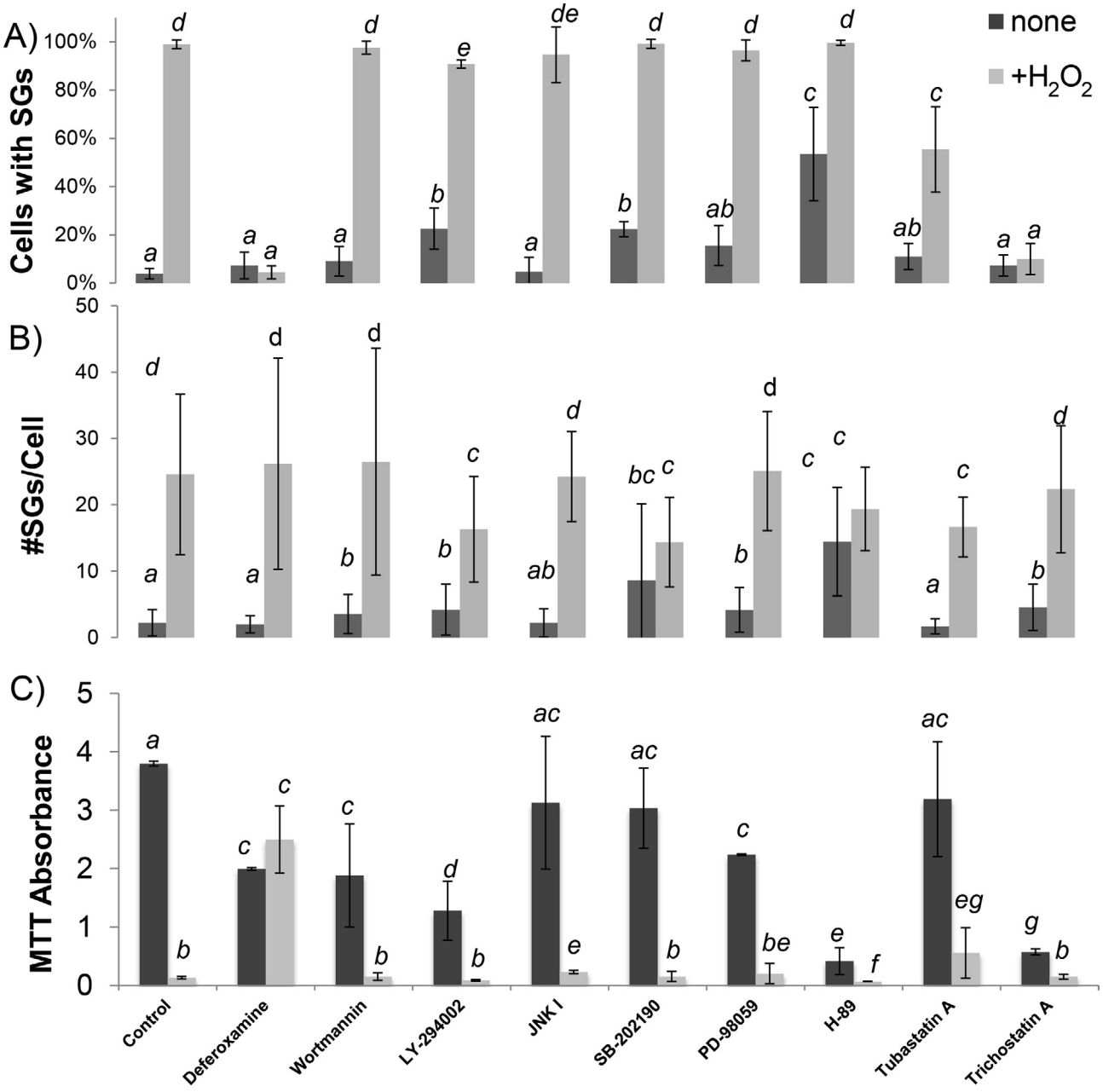

Fig. 5. Effect of Pharmacological Inhibitors on SG Induction by H_2O_2. HeLa cells were incubated with pharmacological inhibitors 1 h prior to 2-hours treatment with 400 μM H_2O_2 (A, B) or 800 μM H_2O_2 (C) The doses of pharmacological inhibitor are: Deferoxamine, 50 μM; Wortmannin, 40 μM; LY-204002, 40 μM; JNK Inhibitor I, 12 μM; SB-202190, 30 μM; PD-98059, 80 μM; H-89, 30 μM; Tubastatin A, 10 μM; and Trichostatin A, 10 μM. Cells were fixed after 2 h of H_2O_2 treatment for immunocytochemistry to stain for TIA-1 (A, B) or changed to fresh culture medium containing 10% FBS for 16 h before MTT assay as described in the Methods (C). About 300 cells in random fields were counted for each sample under a fluorescence microscope with 60 × objective lens for calculating the percentage of cells containing SGs (A). 15 (control), 30 (inhibitor alone) or 50 (H_2O_2 without or with inhibitor) cells containing stress SGs were counted for the number of SGs per cell (B). The data of means ± standard deviations were obtained from one experiment representative of 3 replicate experiments, and were used for statistical analysis by ANOVA, and verified by Student's *t*-test assuming unequal variances. Different letters indicate significant differences between the means of groups ($p < 0.05$). The means labeled with "*a*" are significantly different from that labeled with "*b*", "*c*", "*d*", "*e*", "*f*" or "*g*", whereas two letters, e.g. "*ab*" indicate no significant difference that labeled with "*a*" or "*b*".

formation. Aulas et al. (2017) tested a variety of stressors and found that oxidative stress and hyperosmotic stress being most effective for inducing SGs compared to heat shock, ER stress, proteasome inhibition, UV radiation or inhibition of eIF4A. While H89 can be added to the list of SG inducers, oxidants are most effective for SG induction, therefore remaining the top choice for studying the mechanism of SG formation.

SG formation serves as an antagonistic mechanism against apoptosis (Takahashi et al., 2013). Although PI3K/Akt pathway has been reported as an important pathway for cell survival; PI3K inhibitors did not affect the percentage of cells containing SGs following H_2O_2 treatment. However, a trend of decrease in the number of SGs per cell was observed with LY-294002 (Fig. 5B). Since mTOR complex downstream of PI3K/Akt inhibits the assembly of autophagosomes, inhibi-

tion of PI3K/Akt results in increased autophagosome formation, providing a possible explanation for the observed decrease in the number of SGs per cell with LY-294002. A second possibility is related to the report showing mTOR-S6 kinase promotes SG assembly due to eIF2a phosphorylation by S6 kinase 1 (Sfakianos et al., 2018). Inhibition of PI3K/Akt leads to S6 kinase 1 inhibition and therefore reduction of SG formation.

The role of MAPKs in SG assembly is controversial. Consistent with our finding, JNK inhibition did not affect oxidative stress induced SGs as measured by RNA binding protein HuR as a biomarker of SGs (Meyerowitz et al., 2011;6:57.). Although p38 MAPK inhibitor did not affect the percentage cells containing SGs following H_2O_2 treatment, a downward trend was observed in the number of SGs per cell in those cells containing SGs, to the level similar to that with LY-294002 (Fig. 5B). A well-established signaling pathway for SG formation is 5′-AMP-activated protein kinase (AMPK) (Mahboubi et al., 2016, 2015). Since p38 activation can be a downstream event of AMPK, there is a possibility that p38 MAPK mediates the interplay between AMPK and SGs.

Trichostatin A is a broad HDAC inhibitor, can inhibit HDAC6 as well as nuclear HDACs. HDAC6 has been shown to play a role in SG biology during arsenite stress or T-cell leukemia virus infection (Kwon et al., 2007; Legros et al., 2011). Association with G3BP and deacetylation of α -tubulin appear to mediate SG formation (Mahboubi et al., 2016; Kwon et al., 2007). Our data from Tubastatin A is consistent with a role of HDAC6 in oxidants induced SGs (Fig. 5), related to the fact that HDAC6 regulates microtubule assembly and fusion of microscale SGs along the microtubules to produce microscopically visible SGs. Compared to Tubastatin A, Trichostatin A is 300 fold more selective for class IIa nuclear HDACs than cytoplasmid HDACs (Lobera et al., 2013). Little is known about the role of class IIa HDACs in SG formation. Functionally, an inhibitory effect of Trichostatin A in H_2O_2 induced SGs does not translate to an increase in cell death (data not shown). Since the process of SG formation requires ATP, there is a possibility that inhibition of metabolic activity by Trichostatin A may compound its effect on HDAC inhibition for effective blockage of SG formation.

Declaration of Competing Interest

The authors declare that they have no known competing financial interests or personal relationships that could have appeared to influence the work reported in this paper.

Acknowledgements

Research works under Dr. Qin M. Chen's direction have been supported by NIH R01 GM111337, R01 GM125212, R01 GM126165, Holsclaw Endowment, and The University of Arizona College of Pharmacy start-up fund.

Funding source

2014-2018, NIH R01 GM111337 "Translational Control of Oxidative Stress"

2018-2022, NIH R01 GM125212A1 "Mechanism and Function of Stress Induced Protein Translation"

2018-2022, NIH R01 GM126165A1 "Nrf2 Protein Translation for Protection Against Tissue Injury"

References

Anderson, P., Kedersha, N., 2008. Stress granules: the Tao of RNA triage. Trends Biochem. Sci. 33 (3), 141–150.

Aulas, A., Fay, M.M., Lyons, S.M., Achorn, C.A., Kedersha, N., Anderson, P., Ivanov, P., 2017. Stress-specific differences in assembly and composition of stress granules and related foci. J. Cell Sci. 130 (5), 927–937.

Barr, R.K., Boehm, I., Attwood, P.V., Watt, P.M., Bogoyevitch, M.A., 2004. The critical features and the mechanism of inhibition of a kinase interaction motif-based peptide inhibitor of JNK. J. Biol. Chem. 279 (35), 36327–36338.

Barthel, A., Klotz, L.O., 2005. Phosphoinositide 3-kinase signaling in the cellular response to oxidative stress. Biol. Chem. 386 (3), 207–216.

Buchan, J.R., Kolaitis, R.M., Taylor, J.P., Parker, R., 2013. Eukaryotic stress granules are cleared by autophagy and Cdc48/VCP function. Cell 153 (7), 1461–1474.

Buchan, J.R., Parker, R., 2009. Eukaryotic stress granules: the ins and outs of translation. Mol. Cell 36 (6), 932–941.

Butler, K.V., Kalin, J., Brochier, C., Vistoli, G., Langley, B., Kozikowski, A.P., 2010. Rational design and simple chemistry yield a superior, neuroprotective HDAC6 inhibitor, tubastatin A. J. Am. Chem. Soc. 132 (31), 10842–10846.

Coronella-Wood, J., Terrand, J., Sun, H., Chen, Q.M., 2004. c-Fos phosphorylation induced by H2O2 prevents proteasomal degradation of c-Fos in cardiomyocytes. J. Biol. Chem. 279 (32), 33567–33574.

Davies, S.P., Reddy, H., Caivano, M., Cohen, P., 2000. Specificity and mechanism of action of some commonly used protein kinase inhibitors. Biochem. J. 351 (Pt 1), 95–105.

Droge, W., 2002. Free radicals in the physiological control of cell function. Physiol. Rev. 82 (1), 47–95.

Drummond, D.C., Noble, C.O., Kirpotin, D.B., Guo, Z., Scott, G.K., Benz, C.C., 2005. Clinical development of histone deacetylase inhibitors as anticancer agents. Annu. Rev. Pharmacol. Toxicol. 45, 495–528.

Gilks, N., Kedersha, N., Ayodele, M., Shen, L., Stoecklin, G., Dember, L.M., Anderson, P., 2004. Stress granule assembly is mediated by prion-like aggregation of TIA-1. Mol. Biol. Cell 15 (12), 5383–5398.

Gopalakrishna, R., Jaken, S., 2000. Protein kinase C signaling and oxidative stress. Free Radical Biol. Med. 28 (9), 1349–1361.

Jain, S., Wheeler, J.R., Walters, R.W., Agrawal, A., Barsic, A., Parker, R., 2016. ATPase-modulated stress granules contain a diverse proteome and substructure. Cell 164 (3), 487–498.

Kappeler, K.V., Zhang, J., Dinh, T.N., Strom, J.G., Chen, Q.M., 2012. Histone deacetylase 6 associates with ribosomes and regulates de novo protein translation during arsenite stress. Toxicol. Sci. 127 (1), 246–255.

Kedersha, N., Chen, S., Gilks, N., Li, W., Miller, I.J., Stahl, J., Anderson, P., 2002. Evidence that ternary complex (eIF2-GTP-tRNA(i)(Met))-deficient preinitiation complexes are core constituents of mammalian stress granules. Mol. Biol. Cell 13 (1), 195–210.

Kedersha, N.L., Gupta, M., Li, W., Miller, I., Anderson, P., 1999. RNA-binding proteins TIA-1 and TIAR link the phosphorylation of eIF-2 alpha to the assembly of mammalian stress granules. J. Cell Biol. 147 (7), 1431–1442.

Kwon, S., Zhang, Y., Matthias, P., 2007. The deacetylase HDAC6 is a novel critical component of stress granules involved in the stress response. Genes Dev. 21 (24), 3381–3394.

Legros, S., Boxus, M., Gatot, J.S., Van Lint, C., Kruys, V., Kettmann, R., Twizere, J.C., Dequiedt, F., 2011. The HTLV-1 tax protein inhibits formation of stress granules by interacting with histone deacetylase 6. Oncogene 30 (38), 4050–4062.

Lobera, M., Madauss, K.P., Pohlhaus, D.T., Wright, Q.G., Trocha, M., Schmidt, D.R., Baloglu, E., Trump, R.P., Head, M.S., Hofmann, G.A., 2013. Selective class IIa histone deacetylase inhibition via a nonchelating zinc-binding group. Nat. Chem. Biol. 9 (5), 319–325.

Mahboubi, H., Barise, R., Stochaj, U., 2015. 5'-AMP-activated protein kinase alpha regulates stress granule biogenesis. Biochim. Biophys. Acta, Mol. Cell. Biol. Lipids 1853 (7), 1725–1737.

Mahboubi, H., Stochaj, U., 2017. Cytoplasmic stress granules: Dynamic modulators of cell signaling and disease. Biochim. Biophys. Acta, Mol. Cell. Biol. Lipids 1863 (4), 884–895.

Mahboubi, H., Koromilas, A.E., Stochaj, U., 2016. AMP kinase activation alters oxidant-induced stress granule assembly by modulating cell signaling and microtubule organization. Mol. Pharmacol. 90 (4), 460–468.

Markmiller, S., Soltanieh, S., Server, K.L., Mak, R., Jin, W., Fang, M.Y., Luo, E.C., Krach, F., Yang, D., Sen, A., 2018. Context-dependent and disease-specific diversity in protein interactions within stress granules. Cell 172 (3), 590–604 e13.

Martin, S., Tazi, J., 2014. Visualization of G3BP stress granules dynamics in live primary cells. J. Vis. Exp. 87.

Matsuzawa, A., Ichijo, H., 2008. Redox control of cell fate by MAP kinase: physiological roles of ASK1-MAP kinase pathway in stress signaling. Biochim. Biophys. Acta, Mol. Cell. Biol. Lipids 1780 (11), 1325–1336.

McCormick, C., Khaperskyy, D.A., 2017. Translation inhibition and stress granules in the antiviral immune response. Nat. Rev. Immunol. 17 (10), 647–660.

Meyerowitz, J., Parker, S.J., Vella, L.J., Ng, D., Price, K.A., Liddell, J.R., Caragounis, A., Li, Q.X., Masters, C.L., Nonaka, T., et al, 2011. C-Jun N-terminal kinase controls TDP-43 accumulation in stress granules induced by oxidative stress. Mol. Neurodegener. 6, 57.

Miura, K., Taura, K., Kodama, Y., Schnabl, B., Brenner, D.A., 2008. Hepatitis C virus-induced oxidative stress suppresses hepcidin expression through increased histone deacetylase activity. Hepatology 48 (5), 1420–1429.

Mochly-Rosen, D., Das, K., Grimes, K.V., 2012. Protein kinase C, an elusive therapeutic target?. Nat Rev Drug Discov 11 (12), 937–957.

Panas, M.D., Ivanov, P., Anderson, P., 2016. Mechanistic insights into mammalian stress granule dynamics. J. Cell Biol. 215 (3), 313–323.

Protter, D.S., Parker, R., 2016. Principles and properties of stress granules. Trends Cell Biol. 26 (9), 668–679.

Sfakianos, A.P., Mellor, L.E., Pang, Y.F., Kritsiligkou, P., Needs, H., Abou-Hamdan, H., Desaubry, L., Poulin, G.B., Ashe, M.P., Whitmarsh, A.J., 2018. The mTOR-S6 kinase pathway promotes stress granule assembly. Cell Death Differ..

Souquere, S., Mollet, S., Kress, M., Dautry, F., Pierron, G., Weil, D., 2009. Unravelling the ultrastructure of stress granules and associated P-bodies in human cells. J. Cell Sci. 122 (Pt 20), 3619–3626.
Sugden, P.H., Clerk, A., 2006. Oxidative stress and growth-regulating intracellular signaling pathways in cardiac myocytes. Antioxid. Redox Signal. 8 (11–12), 2111–2124.
Takahashi, M., Higuchi, M., Matsuki, H., Yoshita, M., Ohsawa, T., Oie, M., Fujii, M., 2013. Stress granules inhibit apoptosis by reducing reactive oxygen species production. Mol. Cell. Biol. 33 (4), 815–829.
Tu, V., Bahl, J., Chen, Q., 2002. Signals of oxidant-induced hypertrophy of cardiac myocytes: key activation of phosphatidylinositol 3-kinase and p70S6 kinase. J. Pharm. Exp. Therap. 300 (3), 1101–1110.
Tu, V., Chen, Q., 2003. Distinct roles of ERKs and p38 MAPK in oxidant induced cardiomyocyte hypertrophy. Cardiovasc. Tox 3 (2), 119–133.
Yakes, F.M., Van Houten, B., 1997. Mitochondrial DNA damage is more extensive and persists longer than nuclear DNA damage in human cells following oxidative stress. Proc. Natl. Acad. Sci. 94 (2), 514–519.
Zelko, I.N., Folz, R.J., 2015. Regulation of oxidative stress in pulmonary artery endothelium. modulation of extracellular superoxide dismutase and nox4 expression using histone deacetylase class I inhibitors. Am. J. Respir. Cell Mol. Biol. 53 (4), 513–524.